

Remote sensing of tidal chlorophyll-a variations in estuaries

GLENN P. CATTS[†] and SIAMAK KHORRAM

North Carolina State University, Raleigh,
North Carolina 27695-7106, U.S.A.

JAMES E. CLOERN

U.S. Geological Survey, Menlo Park, California 94025, U.S.A.

ALLEN W. KNIGHT

University of California, Davis, California, U.S.A.

and STEPHEN D. DEGLORIA

University of California, Berkeley, California 94720, U.S.A.

(Received 19 July 1984; in final form 3 January 1985)

Abstract. Simultaneous acquisition of surface chlorophyll-a concentrations for 39 samples from boats and Daedalus 1260 Multispectral Scanner data from a U-2 aircraft was conducted in the northern reaches of San Francisco Bay on 28 August 1980. These data were used to develop regression models for predicting surface chlorophyll-a concentrations over the study area for ebb-tide (8.40 a.m. P.D.T. (Pacific Daylight Time)) and flood-tide (3.10 p.m. P.D.T.) conditions. After selection of a single 'best fitting' model for both morning and afternoon data sets, the chlorophyll-a concentration was predicted for ebb and flood tide for the entire study area at approximately 40 m x 40 m resolution. The predicted spatial display of chlorophyll-a revealed a localized area of high phytoplankton biomass that has been inferred from field surveys and appears to be a common summer phenomenon.

Knowledge of the distribution of phytoplankton and the location of this zone of high biomass is valuable in establishing management policies for this ecologically important estuary. Furthermore, the techniques used here may provide an alternative cost-effective method for assessing water-quality conditions and they may prove useful for studying spatial variations (patchiness) and seasonal variations in phytoplankton biomass in other estuaries and coastal waters.

1. Introduction

Estuaries are dynamic water bodies characterized by temporal changes that occur over a spectrum of scales, ranging from short-term (hourly) variations driven primarily by tidal currents to long-term (seasonal or interannual) variations caused by changes in meteorological forcings or river discharge. Estuaries are also spatially heterogeneous and often have large horizontal (or vertical) gradients in water properties (e.g. salinity, suspended sediments, phytoplankton biomass) that result from local variations in bathymetry, circulation and mixing, or sources/sinks of dissolved and suspended constituents. Knowledge of mechanisms that cause spatio-temporal heterogeneity in estuaries is based in large part upon the results of *in situ* sampling that is costly (both in time and money) and often inefficient, particularly if sampling is required over a large geographical area and over more than one time scale. Truly synoptic measurements

[†] Glenn P. Catts is now with the U.S. Forest Service at Fort Collins, Colorado.

from boats are nearly impossible in estuaries having rapid (100–200 cm/s) tidal currents. If specific properties of estuarine waters can be measured accurately using remote-sensing techniques, then understanding of mechanisms through which physical processes (tidal advection, estuarine not-tidal circulation, horizontal dispersion, resuspension) effect change in dynamic estuarine waters can be improved.

This general problem is exemplified by the need for better understanding of mechanisms that control phytoplankton dynamics in the northern San Francisco Bay estuary, which has been the focus of intensive field investigation during the past decade (Conomos 1979). The upper reach of San Francisco Bay (Suisun Bay, figure 1) comprises of two deep (~ 10 – 15 m) channels and a shallow (~ 1 – 2 m) embayment and is the site of local accumulations of suspended particulates (a turbidity maximum) (Conomos and Peterson 1977) and phytoplankton (a chlorophyll maximum) (Peterson *et al.* 1975) during summer. The turbidity maximum, a common feature of partially mixed estuaries (Postma 1967, Meade 1972), results from two physical processes: particle sinking and estuarine circulation, such that residual (tidally averaged) surface currents flow seaward while bottom currents flow landward. The result is a trapping mechanism that retains suspended particulates in that region of the estuary (null zone) where the landward bottom current converges with the seaward river current. These same physical processes apparently also operate on phytoplankton cells (mostly diatoms) in Suisun Bay and act to retain phytoplankton biomass that is produced over the shoals, where light availability is sufficient to sustain net photosynthesis and growth (Cloern and Cheng 1981, Cloern *et al.* 1983). These concepts have evolved from measurements made over a coarse grid of stations that is sampled on weekly time scales or longer. Hence, we know little about small-scale (less than about 2 km) spatial heterogeneity (phytoplankton patchiness, including that associated with fronts), short-term (hourly or daily) variations in structure of the phytoplankton maximum or rates of horizontal mixing of water masses between the shoals (the source of phytoplankton biomass) and deeper channels. If remotely sensed images could accurately represent the horizontal distribution of phytoplankton biomass in turbid shallow waters, then the dynamic nature of the phytoplankton maximum of Suisun Bay and other estuaries may become more clear.

Further, San Francisco Bay, like many urbanized estuaries, is subjected to perturbations (dredging, marsh reclamation, diversions of freshwater inflow, waste discharges) that potentially alter water quality; remote sensing may be a valuable tool for monitoring the long-term ecological consequences of such perturbations. The purpose of this study is to examine the potential utility of high-resolution multispectral imagery, similar to that provided by the **LANDSAT-4** Thematic Mapper (TM), for mapping the spatial distribution of phytoplankton biomass (chlorophyll-a) in the upper reach of northern San Francisco Bay.

2. Objectives

Specific objectives were to determine:

- (1) Whether remotely sensed reflectance data from a scanner similar to the TM sensor can be used to map surface chlorophyll-a accurately in a shallow turbid environment.
- (2) Which spectral bands are required for mapping chlorophyll in turbid estuaries.
- (3) What statistical model(s) accurately describe chlorophyll concentration.
- (4) Whether statistical models are conservative over short time scales (i.e. are model parameters constant over a tidal cycle).

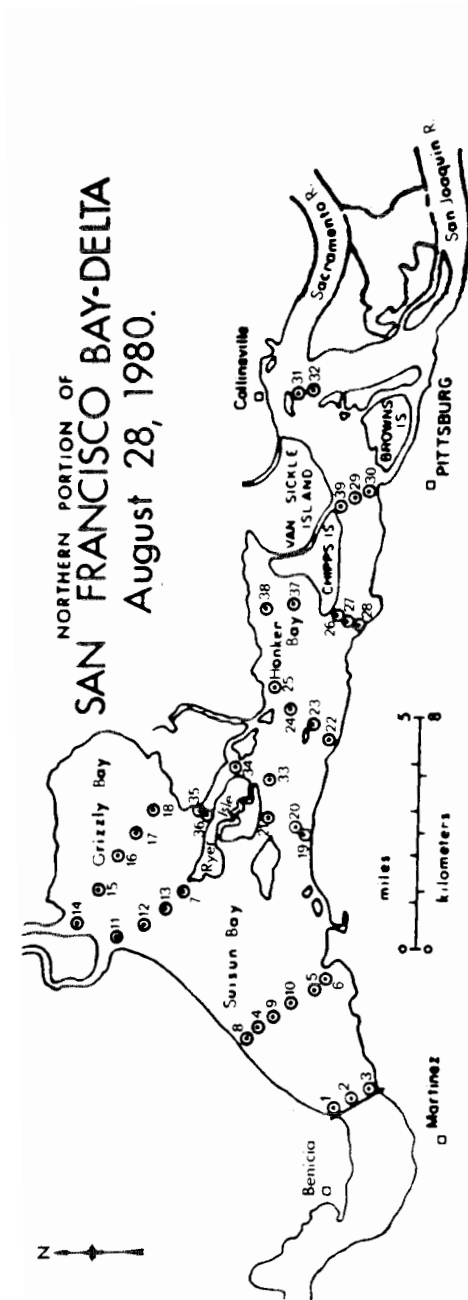


Figure 1 The study area in the northern portion of the San Francisco Bay delta showing 39 sample site locations used on 28 August 1980.

3. Brief review of work done previously

Mapping chlorophyll-a from interpolation among surface measurements is a difficult task, subjective at best, and some sampling stations are too shallow to permit easy access for sampling (Khorram 1981 a). As an alternative to interpolation among surface measurements, Khorram (1981 a) first used Ocean Colour Scanner (OCS) data acquired from a NASA U-2 overflight with simultaneous surface measurements to delineate the chlorophyll maximum in northern San Francisco Bay. Khorram (1981 b) later used LANDSAT-3 Multispectral Scanner (MSS) digital data, along with concurrent surface measurements, to map other indices of water quality over the entire San Francisco Bay. Both studies successfully delineated the turbidity/chlorophyll maximum and LANDSAT-assisted mapping provided a potential for repetitive monitoring coverage of the entire San Francisco Bay. However, some concern has arisen (among government officials) over the relatively low resolution capability (80 m x 10 m) of the LANDSAT MSS system. In response to this concern, this research has employed a higher resolution Daedalus 1260 MSS (40 m x 40 m), capable of recording better than twice as many wavelength channels (10 channels) over the same spectral range as the LANDSAT-3 MSS (four channels), table 1. Narrowing the receiving wavelength ranges facilitates remote sensing of specific absorption and reflectance spectra characteristics of chlorophyll-a.

Coastal chlorophyll-a concentrations may range as high as 1000 $\mu\text{g}/\text{l}$ during bloom conditions (Munday and Zubkoff 1981). Therefore, previous remote-sensing investigations of chlorophyll-a in coastal environments have utilized chlorophyll-a absorbance and reflectance information in the red (670 nm) and near infrared (750 nm) as well as blue and green portions of the electromagnetic spectrum (Johnson 1978, Kim *et al.* 1980, Uno *et al.* 1980, Grew 1981, Johnson *et al.* 1981, Munday and Zubkoff 1981, Bowker *et al.* 1983).

No data on the concentration of suspended sediments in each chlorophyll-a surface sample are available for this study. It is highly probable, therefore, that suspended sediments may be influencing scanner radiance measurements in Daedalus 1260 channels 7 and 8. According to Morel and Prieur (1977) suspended sediment reflectance in wavelengths regions of channels 7 and 8 are quantitatively similar. By the use of a ratio of channel 7 over channel 8 it is hoped that the radiance contribution from suspended sediments will be minimized.

A further note of interest is that in the aforementioned references to remote-sensing studies, only one sample size exceeded 25 sites. This sparse number of surface samples

Table 1. Daedalus MSS, channel wavelength ranges.

Channel	Wavelength (nm)	Colour, etc.
1	380-420	Ultraviolet
2	420-450	Violet
3	450-500	Blue
4	500-550	Green
5	550-600	Yellow
6	600-650	Orange
7	650-690	Red
8	700-790	Infrared
9	800-890	Infrared
10	920-1100	Infrared

is characteristic of remote-sensing water-quality investigations due to logistic and expense.

4. Considerations in the selection of wavelength regions used for modelling

The physical basis for the models developed in this study was derived from inspecting the literature on laboratory investigations of the spectral characteristics of phytoplankton, as well as previously successful remote-sensing investigations of estuarine chlorophyll-a.

Previous laboratory research has shown that the spectral characteristics of phytoplankton cultures depend on age, vitality and concentration as well as taxonomic distinction (Wilson and Kiefer 1979, Uno *et al.* 1980). All algae absorb energy in the 430 and 670–680 nm regions of the electromagnetic spectrum due to the presence of chlorophyll-a (Anderson and Horne 1975). Reported laboratory spectral curves of marine diatoms, including the dominant species of the study date, *Skeletonema costatum*, demonstrate that as chlorophyll-a concentration increases, wavelengths of 500 and 670 nm are increasingly absorbed while wavelengths in the 550–600 nm range and near-infrared spectral region (750 nm) are increasingly reflected (Anderson and Horne 1975, Uno *et al.* 1980), see figure 2.

Recent work at NASA Langley Research Center (Farmer *et al.* 1983) involved investigations into the use of visible absorbance spectra as a basis for remote sensing of algal concentration and community composition. They found that absorbance spectra of different cultures of the same species were most similar. The separation and quantification of mixed phytoplankton colour groups was possible using information from the difference between radiance measured at 680 and 720 nm (Daedalus channels 7 and 8).

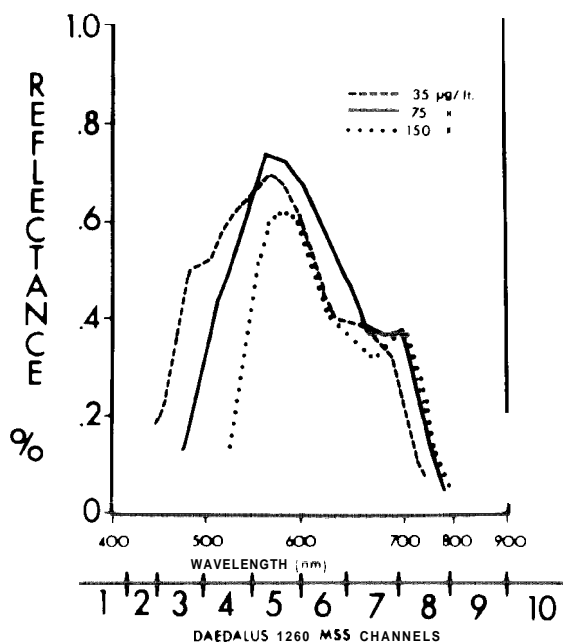


Figure 2. Relationship between percentage reflectance and wavelength at various concentrations of *Skeletonema costatum* in culture (adapted from Uno *et al.* 1980).

The selection of Daedalus channel ratio 7/8 as an independent variable in the chlorophyll-a model is based on the aforementioned spectral properties of chlorophyll-a. As chlorophyll-a concentration increases in surface waters, the energy is increasingly absorbed in Daedalus channel 7 (650–690 nm). On the other hand, with increasing chlorophyll-a concentration, the reflectance in Daedalus channel 8 (700–790 nm) increases. It is the change in the slope of the reflectance curve from Daedalus channel 7 to Daedalus channel 8 with increasing chlorophyll-a concentration that permits the ratio of 7/8 to be a useful predictor variable. This 7/8 ratio is most useful at higher chlorophyll-a concentrations due to the increasing absorption of near-infrared radiation by water reducing the intensity of the reflectance by chlorophyll-a in Daedalus channel 8 when the concentration of chlorophyll-a is low (Morel and Prieur 1977, Gordon and Clark 1980, Uno et al. 1980). To observe the increase in the value of the channel 7 over 8 ratio as chlorophyll-a concentration decreases see the third and eighth columns of tables 2 and 3.

The absorption in the blue and green wavelength regions of the spectrum (450–550 nm) by chlorophyll-a is selected as an input variable in the model because this absorption is sensitive to changes in chlorophyll-a at lower concentrations (Uno et al. 1980). The form of this variable, Daedalus channel 3 minus Daedalus channel 10, is an attempt to remove unwanted reflectance contributions from the atmospheric haze that plagued the afternoon scene. The rationale of this transformation is that most of the energy recorded by Daedalus channel 10 is atmospheric or surface reflectance since essentially near zero reflectance from the water column would occur in this wavelength region of 1000–1100 nm (Yentsch 1960, Morel and Prieur 1977, Gordon and Clark 1980). At the same time, absorption by chlorophyll-a is taking place in Daedalus channels 2, 3 and 4 (Anderson and Horne 1975, Uno et al. 1980). As chlorophyll-a concentration increases, the slope between reflectance values in Daedalus channels 2 and 4 moves in a positive direction (Uno et al. 1980). Channel 2 minus 10, channel 3 minus 10 and channel 4 minus 10 were all examined as possible variable transformations during regression modelling. The transformation 3 minus 10 applied most consistently to both morning and afternoon data sets. For this reason, it is concluded that for these particular data the proportion of atmospheric interference in Daedalus channel 3 was removed by subtracting the value of Daedalus channel 10. In any case, development of future models capable of consistent predictions of surface chlorophyll-a concentrations must be based on simultaneous measurements made of surface irradiance (upwelling and downwelling) and scanner spectral value comparisons.

5. Research methodology

The research approach involved (i) simultaneous acquisition of surface measurements of water quality and Daedalus 1260 MSS data, (ii) laboratory analysis of whole water samples from 39 sites, (iii) extraction of digital count values from Daedalus scanner for 39 sample sites, (iv) bad data replacement, (v) development of regression equations relating Daedalus MSS data to chlorophyll-a measurements and (vi) transformation of Daedalus 1260 MSS data through selected best-fit regression models for production of surface chlorophyll-a distributions for the entire study area.

5.1. Collection and laboratory analysis of surface chlorophyll-a samples

On 28 August 1980 chlorophyll-a samples were collected at 39 sites from five boats. The sampling strategy was designed by the technical staff of several government agencies, which have been involved in water-quality sampling over this study area for

Table 2. Morning ebb-tide raw data. Chlorophyll-*a* concentrations ($\mu\text{g/l}$), Daedalus 1260 scanner band count values and band transformations†.

Site	Time from overflight (min)	Observed chlorophyll- <i>a</i>	Daedalus channel 3	Daedalus channel 7	Daedalus channel 8	Daedalus channel 10	Ratio Daedalus channel 7 to channel 8	Daedalus channel 3 minus channel 10
1	0	14.4	43.96	48.28	42.28	27.36	1.14191	16.60
2	0	9.3	44.00	48.92	42.36	27.40	1.15486	16.60
3	5	9.0	44.04	48.20	41.00	27.44	1.17561	16.60
4	45	33.0	44.04	47.56	41.08	25.52	1.15774	18.52
5	25	20.8	44.20	50.40	44.24	27.60	1.13924	16.60
6	35	28.2	44.36	52.44	48.80	30.92	1.07459	13.44
8	40	66.0	44.92	51.64	48.36	29.96	1.06782	14.96
9	50	23.9	44.76	49.64	43.04	26.48	1.15335	18.28
10	63	22.9	44.04	49.60	42.72	25.72	1.16105	18.32
11	-13	60.5	47.04	53.00	51.08	28.96	1.03759	18.08
12	0	49.5	46.00	51.92	48.88	27.84	1.06219	18.16
13	0	24.4	44.96	47.08	39.76	23.00	1.18410	21.96
14	-18	55.7	47.16	51.36	48.96	28.32	1.04902	18.84
15	0	66.0	47.52	52.96	51.04	28.40	1.03762	19.12
17	20	24.8	45.92	50.92	46.68	25.32	1.09083	20.60
18	13	35.8	45.04	51.20	47.44	25.90	1.07926	19.14
19	55	37.8	44.68	51.36	46.16	29.04	1.11265	15.64
20	65	16.4	44.72	51.12	45.80	28.36	1.11616	16.36
21	68	49.5	44.04	50.28	45.92	27.95	1.09495	16.09
22	71	39.9	44.32	52.76	49.52	31.28	1.06543	13.04
23	55	38.5	44.20	52.00	47.32	29.44	1.09890	14.76
24	-13	34.4	44.96	53.88	51.28	31.70	1.05070	13.26
25	0	53.6	44.96	52.40	49.24	30.64	1.06413	14.32
26	58	33.7	44.92	52.24	48.08	32.28	1.08652	12.64
27	50	27.5	45.04	51.76	46.00	31.48	1.12522	13.56
28	-37	27.3	44.76	51.08	46.36	32.12	1.10181	12.64
29	0	26.1	44.04	53.00	49.88	32.84	1.06255	11.20
30	0	17.2	43.16	50.76	45.60	30.36	1.11316	12.80
31	15	14.6	44.04	51.56	44.92	27.88	1.14782	16.16
32	24	11.5	44.12	51.04	44.40	28.00	1.14955	16.12
33	-42	31.6	44.68	51.88	48.12	29.20	1.07814	15.48
34	-28	39.9	44.00	52.00	50.64	30.72	1.02686	13.28
35	20	32.2	44.00	50.00	46.76	27.88	1.06929	16.12
36	31	48.1	44.00	49.52	46.48	27.60	1.06540	16.40
37	24	28.2	45.00	53.88	51.44	32.60	1.04743	12.40
38	38	36.4	45.08	52.84	47.52	29.00	1.11195	16.08
39	-16	22.1	44.00	52.04	48.32	31.70	1.07699	12.30

† Count values were derived by quantizing spectral radiance ($L\lambda$) to 8 bit digital counts.

many years, to represent the various physical and chemical conditions in the Delta adequately. Sampling was continuous throughout the day with each boat responsible for a number of sample sites along a designated transect. All samples were taken from a depth of 3 ft. Location of the sample sites is shown in figure 1. Sampling times were recorded and surface samples occurring at times closest to the Daedalus scanner overflight were used for the development of models. All surface samples were acquired within 1.5 hours of the scanner overflight.

Water samples were collected onto glass fibre filters which were extracted in 95 per cent acetone. Chlorophyll-a concentration was determined fluorometrically (Strickland and Parsons 1972) from acetone extracts. These values were corrected for phaeopigments. Chlorophyll-a concentrations and extracted count values for the 39 sample sites for the morning overflight are displayed in table 2 and for the afternoon overflight in table 3.

5.2. Acquisition and processing of Daedalus MSS data

From 8.30 to 8.45 a.m. and from 3.00 to 3.15 p.m. (P.D.T.) of 28 August 1980 two NASA Ames Research Center U-2 overflights of the study area were flown at approximately 55 000 ft in conjunction with ebb- and flood-tide conditions, respectively. Overflight times corresponded closely with the highest and lowest water conditions of the study area that day (see figure 3.) An altitude of 55 000 ft produced a ground resolution cell of 42 m x 42 m using the Daedalus 1260 MSS (angular resolving power of 2.5 mrad). The MSS recorded 10 channels of reflected energy and two channels of thermal energy. Only the reflected wavelengths were considered in this study (see table 1).

In order to extract the count values of each scene for the corresponding 39 sample sites a second-order polynomial regression equation was developed. This equation regressed control points from USGS topographic maps using a Universal Transverse Mercator (UTM) grid system against the same control point located visually on the imagery. Regression residuals were examined and sample sites were verified visually. In this fashion, scanner imagery was mathematically transformed to conform to the latitudinal and longitudinal co-ordinates of ground sample-site locations.

To ensure the proper location of sample sites, a block of 5 pixels x 5 pixels surrounding each sample site was located and the average count values computed. These mean count values were then used in developing chlorophyll-a prediction models. The squares outlined in figure 4 represent the 5 pixel x 5 pixel blocks (approx. 200 m x 200 m) for sample sites 4, 5, 6, 8, 9, 10, 11, 12, 13 and 14 in Suisun Bay. This averaging procedure was done for both the morning and afternoon scenes. Standard deviations of count values for all wavelength channels in each pixel block ranged from ± 0.4 per cent.

5.3. Bad data replacement

It was not possible to use the previously described method of count-value extraction for the morning ebb-tide scene. During the morning overflight, severe turbulence was encountered causing tilting of the aircraft. This pitch manifests itself on the imagery by slightly altering the ground distance from one scan line to another. This is visible in figure 4 as a scalloped shoreline. Note also the sickle shapes of the normally rectangular moth ball fleet. The turbulence was unsystematic and randomly variable throughout the scene. Attempting to transform this image to mathematically register it with the afternoon scene or a UTM projection was impossible with the

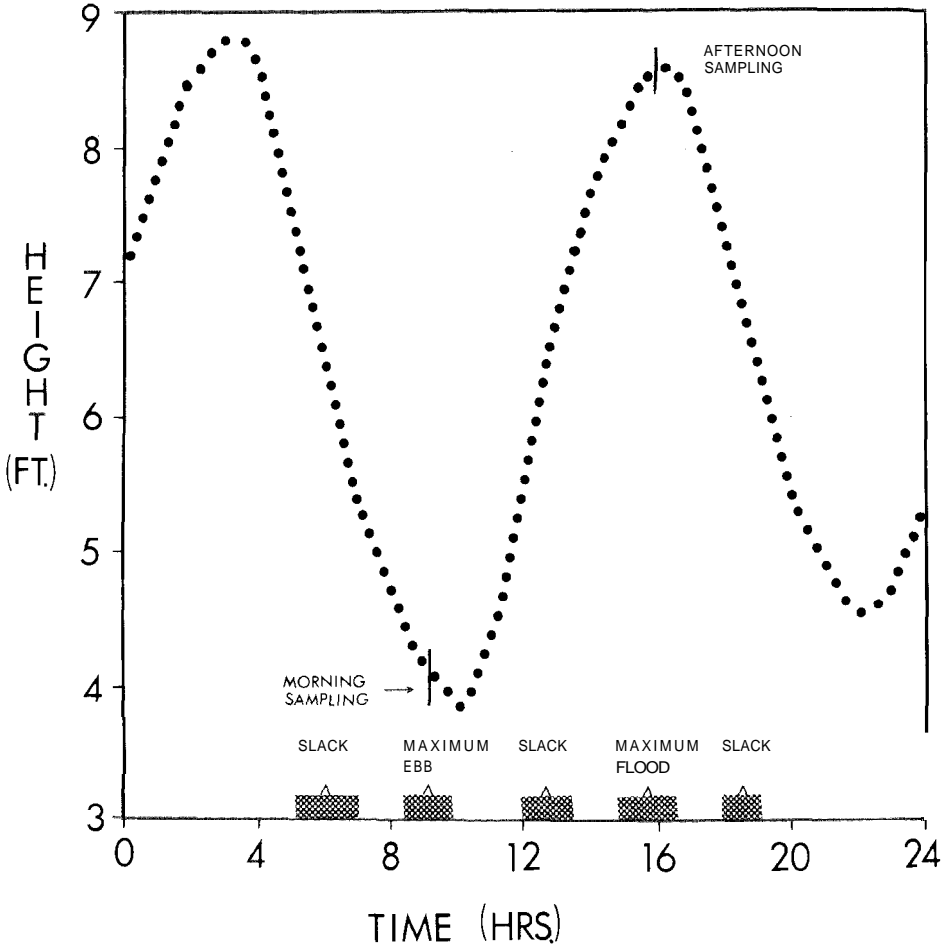


Figure 3. The rise and fall of the tide on the day of sampling within the study area. Vertical lines indicate the approximate time of simultaneous overflight and surface sampling. The dotted line represents water height.

available software. Instead, the sample points were located by triangulation and visual verification techniques. Scan start problems dropped 30 lines of data over Suisun Bay during the morning overflight. Radiance values for two sample sites from the morning scene were lost to this malfunction (sites 7 and 16). Final output products have a black filler region spacing the scene correctly and indicating the area of data loss.

The afternoon scanner overpass had scan line starting problems in Daedalus channel 10. These appear on analogue imagery as lines of offset densities (i.e. land values offset over water and vice versa). An algorithm interpolating across these bad scan values by assigning the average of the preceding and subsequent scan lines to the bad line was used for correction. There were 80 bad scan lines in the morning scene out of 1080 total lines (7.4 per cent).

5.4. Model development

The modelling approach involved two sets (morning and afternoon) of surface measurements and two sets of scanner data. The surface measurements were used as

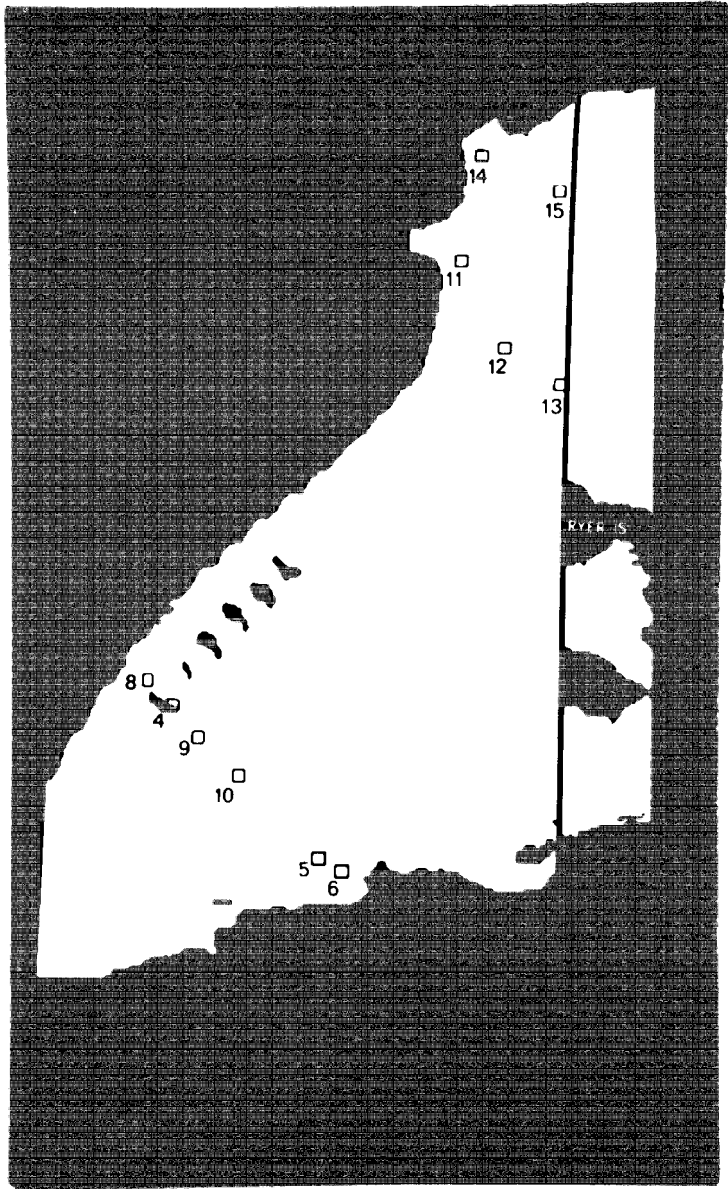


Figure 4. Relative size of 5 pixel x 5 pixel blocks representing 200 m x 200 m on the ground. The discontinuity truncating the western end of the islands at the right is the result of scan dropout region of approximately 30 missing lines. Note image scalloping affecting the northern shoreline of Suisun Bay and the Mothball Fleet.

dependent variables while the independent variables were composed of simple functions of the recorded count values of selected channels of the Daedalus scanner. The 'best fit' single model for predicting chlorophyll-a in both morning and afternoon scenes was chosen on the basis of significance and stability of the overall model and of its (parameters) coefficients. Criteria examined in order to compare various models included R^2 values, F-test results of the significance of the overall model, t-test results

of the significance of the coefficient estimates, standard errors of the overall model and each of its coefficients and residual analysis.

Prior to the use of spectral data in modelling, histograms of the count values for both scenes were examined. The histogram of the morning scene count values appears as a normal distribution while the histogram of the afternoon scene displays a marked bimodal tendency. Upon closer inspection, the bimodal condition of the afternoon scene was attributable to the influences of a thin wedge of haze covering the western third of the imagery and barely detectable on analogue imagery. The haze was thickest (but not visually obstructing) over the westernmost portion of the scene and gradually diminished in thickness until it appeared to be absent east of the three islands in the centre of the scene. Backscattered radiance from the haze gave haze-influenced sites higher count values in all Daedalus MSS channels (see figure 5 and table 4). Daedalus MSS channel 1 (ultraviolet) was removed from analysis due to the extreme degree of atmospheric scattering.

The regression modelling strategy used 30 sample sites from the morning data set ($n = 37$) and 30 sample sites from the afternoon ($n = 39$). These two groups of 30 sites were modelled independently for the purpose of discovering a functional model applicable to both data sets. Seven sites were saved from the morning data for verification of the model and nine sites were saved for verification in the afternoon case. Sites saved for verification were chosen randomly after being stratified by boat location and water depth. The model for the morning ebb tide was

$$\text{Chlorophyll-}a \text{ } (\mu\text{g/l}) = 323.7 + 2.4x_1 - 299.2x_2$$

and for the afternoon flood tide was

$$\text{Chlorophyll-}a \text{ } (\mu\text{g/l}) = 570.8 + 3.1x_1 - 541.2x_2$$

where x_1 is Daedalus channel 3 minus Daedalus channel 10 and x_2 is Daedalus channel 7 divided by Daedalus channel 8.

The summary of modelling and verification regressions appears in table 5. Additionally the model was fitted only to sites where surface measurements were made

Table 4. The mean, standard deviation and range of count values for the 18 haze-influenced and 21 clear sites.

P.M. haze site count values ($N = 18$)				P.M. clear site count values ($N = 21$)			
Daedalus channels	Mean	Standard deviation	Range	Daedalus channel	Mean	Standard deviation	Range
2	99.5	2.45	95.20–94.80	2	85.0	1.65	81.85–88.15
3	60.8	1.79	57.30–64.30	3	51.2	0.72	49.80–52.60
4	76.8	2.00	72.95–80.65	4	65.5	0.81	64.05–66.95
5	66.3	1.62	63.35–69.25	5	57.4	0.83	55.80–59.00
6	66.3	1.70	63.35–69.25	6	57.9	1.13	55.60–60.20
7	73.6	2.39	69.60–77.60	7	62.9	1.23	60.20–65.60
8	74.1	3.63	69.05–79.15	8	61.7	1.97	57.30–66.10
9	55.7	3.03	50.90–60.50	9	45.2	2.03	40.25–50.15
10	61.3	5.46	51.70–70.90	10	46.6	2.61	40.90–52.30

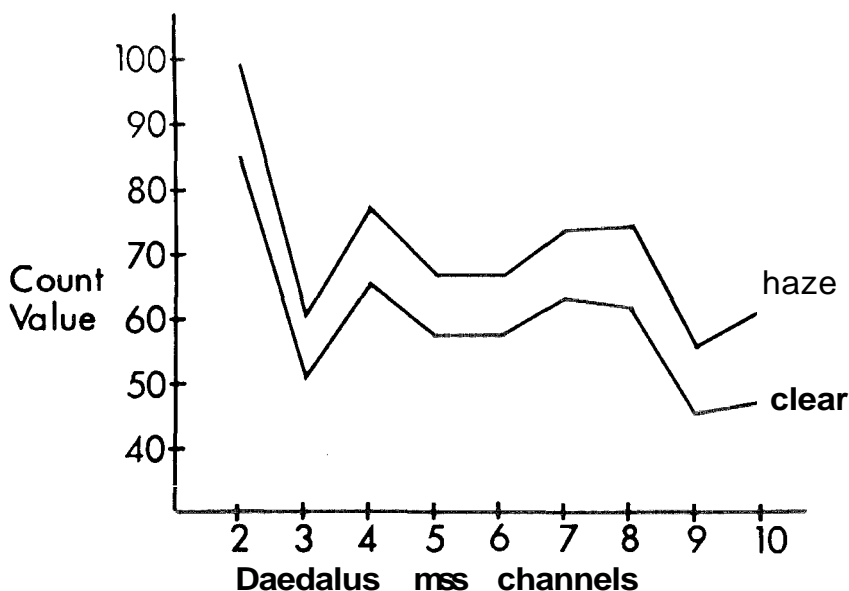


Figure 5. Effect of haze on mean count values of Daedalus channels 2–10 during the afternoon overflight.

within 10 min of the scanner overflight. The necessity for surface measurements to be made as close to the overflight time as possible is demonstrated in the improved fit of these regressions (see table 5). A measure of the percentage variation due to chance (R^2) signifies that in all modelling and verification data sets from 55 to 92 per cent of the variation in the observed chlorophyll-a values can be explained by the models. These models utilize data uncorrected for atmospheric variation. Atmospherically corrected data would improve model performance and aid in developing conservative model coefficients from scene to scene.

Plots of observed versus predicted chlorophyll-u appear in figure 6 for ebb- and flood-tide models developed from 30 sites. Plots of residual versus predicted values appear in figure 7 for these same models. The residual plots display a random dispersion about the residual zero axis and indicate that the variance of predicted chlorophyll-a is constant throughout the predicted range.

5.5. Application of regression models to the entire study area

All morning and afternoon models were displayed for visual inspection of spatial distributions of predicted surface chlorophyll-a concentrations and then compared with interpolated spatial distributions from conventional surface surveys. Models that passed visual inspection were then extended to the entire scene including portions of the estuary not within the study area. Model applications were accomplished by using a simple linear discriminant function. Classification was accomplished by applying this function to each pixel in the study area and then grouping continuous chlorophyll-a surface predictions into discrete classes. These discriminant functions were applied to the Daedalus MSS data to produce classified chlorophyll-u surface concentration maps. These classified maps were then renumbered to produce the final maps (see figure 8).

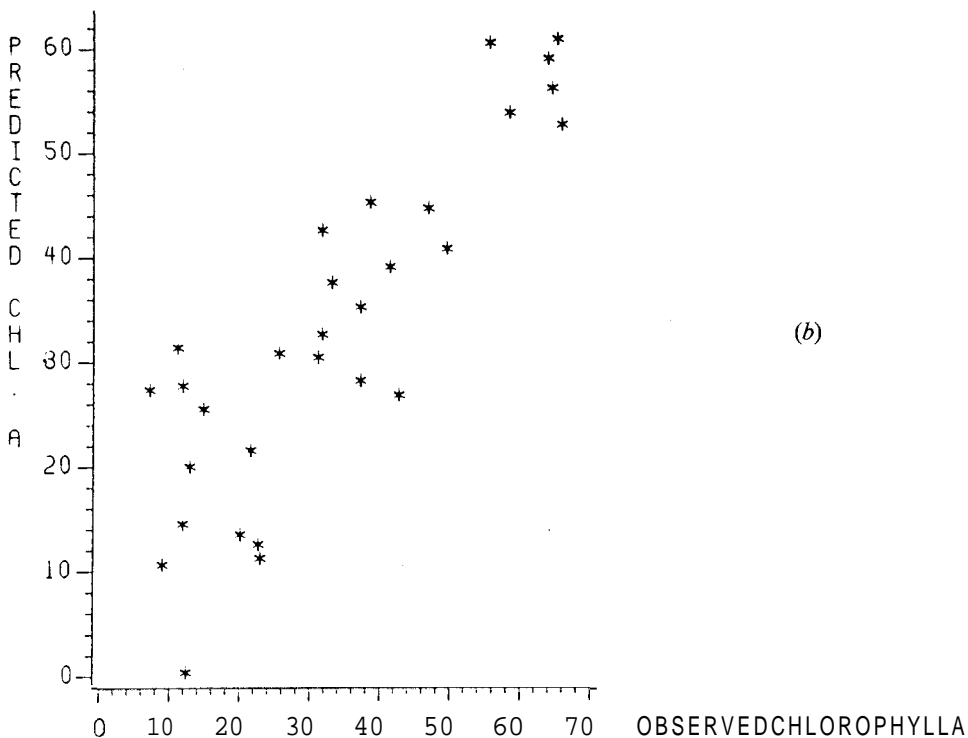
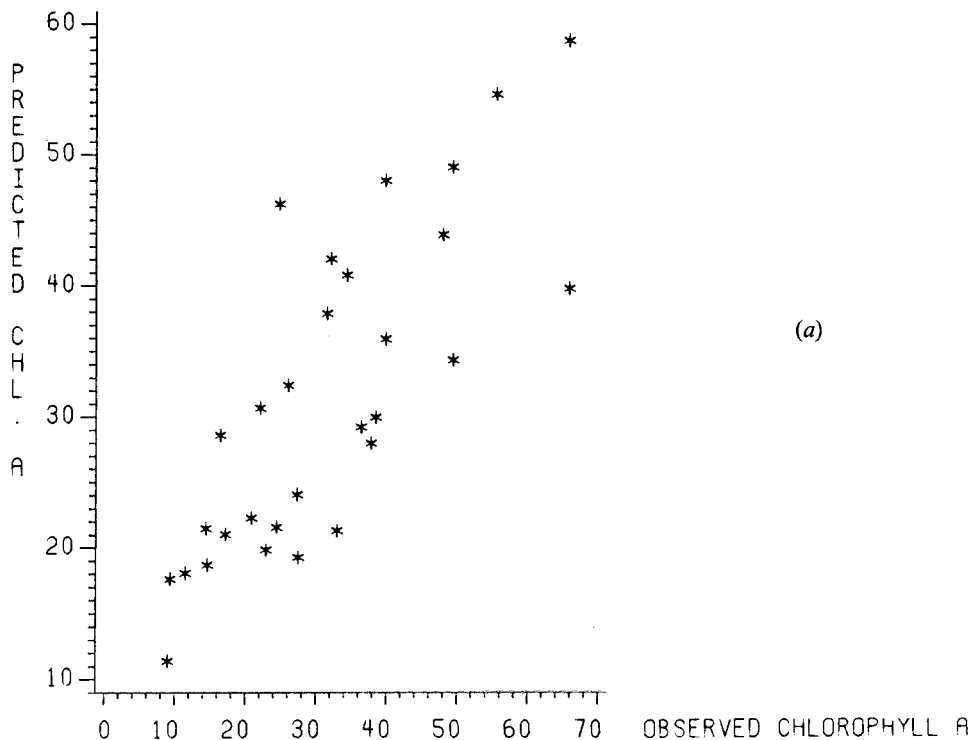
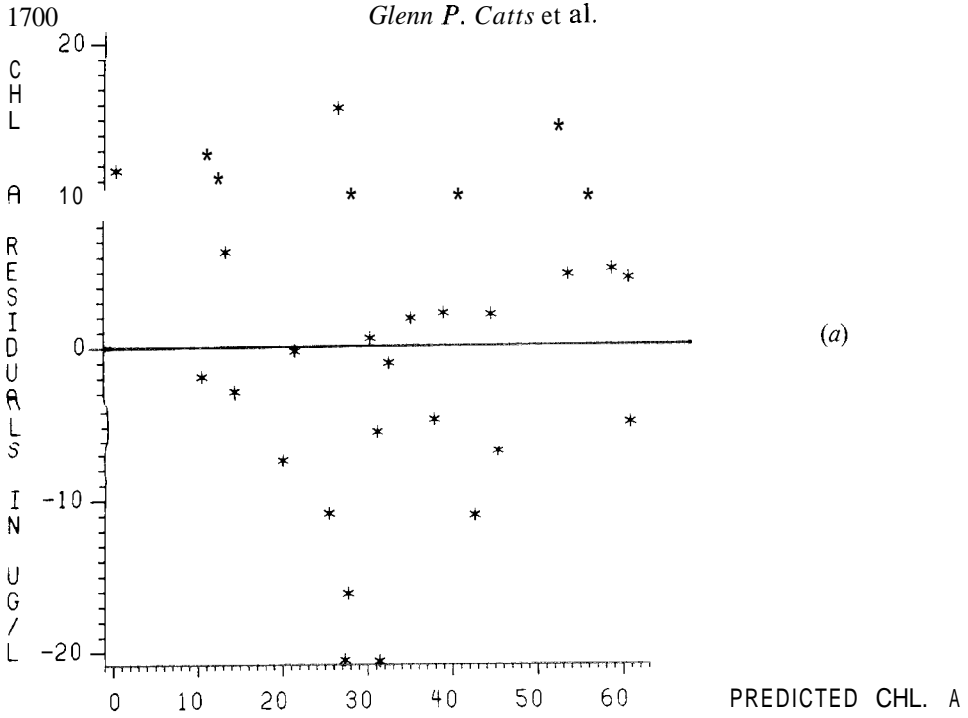


Figure 6. Chlorophyll-a model performance, predicted versus observed chlorophyll-a concentrations ($\mu\text{g/l}$), 28 August 1980, using a 30 sample-site input, (a) morning ebb tide and (b) afternoon flood tide.

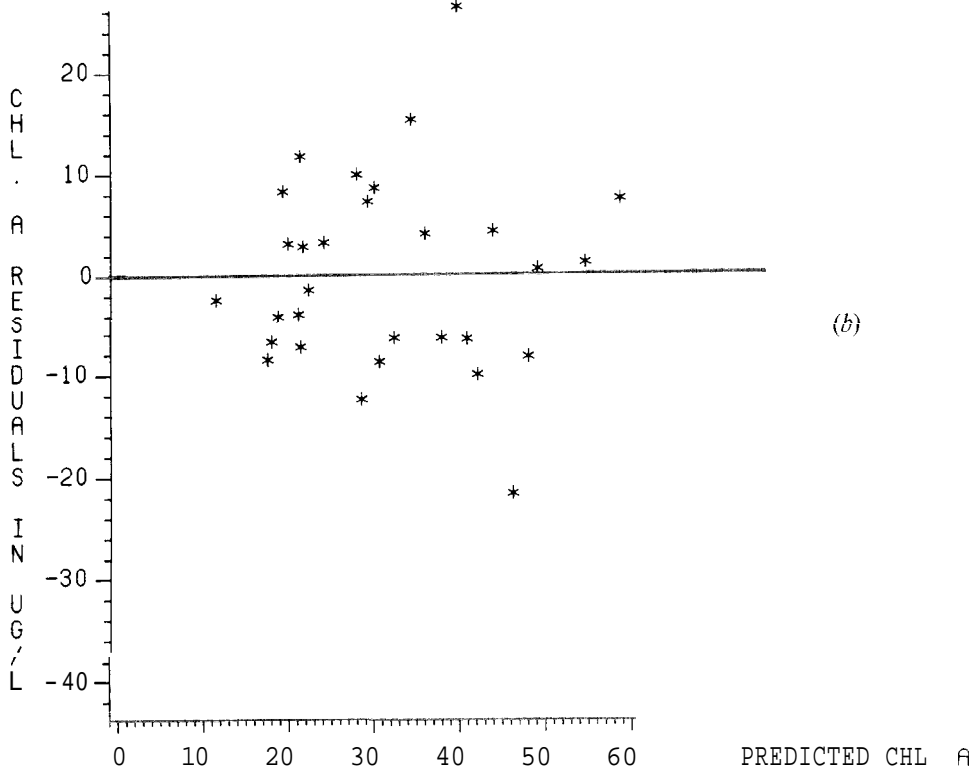
Table 5. Morning ebb-tide results and afternoon flood-tide modelling results.

	R^2	$F/\text{prob} > F$	R.M.S. error	Model coefficients	Coefficient standard error	$\text{Prob} > T $
Morning						
Model development ($n=30$)	0.62	22.4/0.0001	9.872	$a = 323.7$ $b = 2.4$ $c = 299.2$	46.9 0.8 45.0	0.0001 0.0050 0.0001
Model verification ($n=7$)	0.55	2.4/0.2024	11.438	$a = 299.6$ $b = 2.2$ $c = -274.3$	134.7 1.7 130.3	0.0902 0.2658 0.1030
Model using only sites within 10 min of overpass ($n=10$)	0.77	12.2/0.0052	10.669	$a = 369.2$ $b = 2.2$ $c = -340.4$	74.8 1.1 69.8	0.0017 0.0796 0.0018
Afternoon						
Model development ($n=30$)	0.74	39.174/0.0001	9.944	$a = 570.8$ $b = 3.1$ $c = -541.2$	65.7 0.5 65.7	0.0001 0.0001 0.0001
Model verification ($n=9$)	0.93	45.427/0.0002	6.197	$a = 1020.7$ $b = 2.5$ $c = -982.8$	117.0 0.4 116.3	0.0001 0.0007 0.0001
Model using only sites within 10 min of overpass ($n=9$)	0.86	19.526/0.0024	10.116	$a = 666.3$ $b = 1.9$ $c = -629.4$	102.5 0.7 101.8	0.0006 0.0315 0.0008

Model of the form: Chlorophyll- $a = a + bx_1 + cx_2$ ($\mu\text{g/l}$), where x_1 is Daedalus channel 3 minus Daedalus channel 10 and x_2 is Daedalus channel 7 divided by Daedalus channel 8.



(a)



(b)

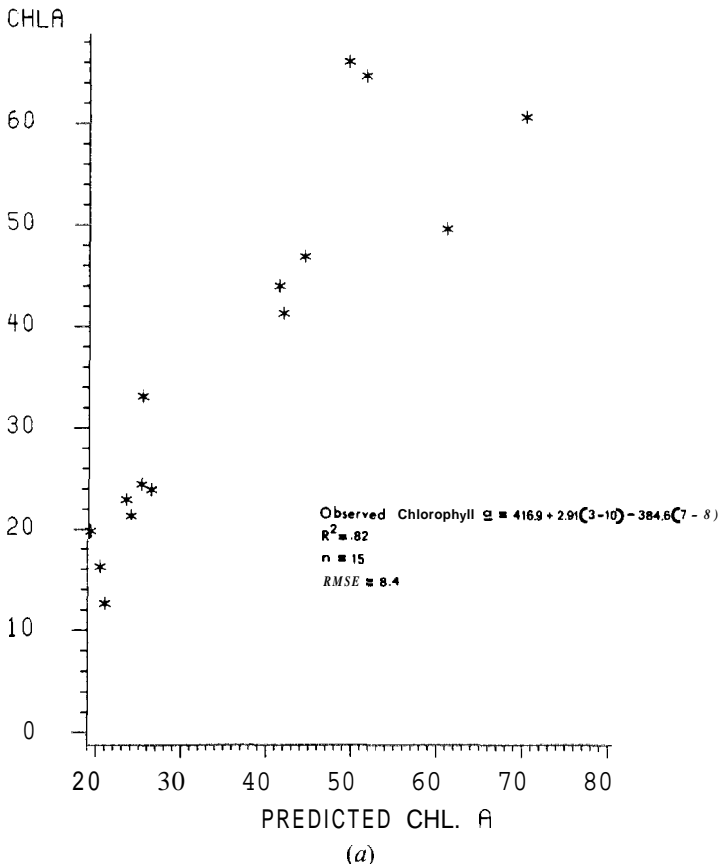
Figure 7. Chlorophyll-a model performance, residual versus predicted chlorophyll-a concentrations ($\mu\text{g/l}$), 28 August 1980, using a 30 sample-site input, (a) morning ebb tide and (b) afternoon flood tide.

6. Discussion of results

The results of this research include:

- (1) A record of chlorophyll-a concentrations determined by laboratory fluorometric analysis for all 39 sample sites during the morning ebb and afternoon flood tide of 28 August 1980.
- (2) A series of statistical models developed from point sample data for the purpose of predicting surface chlorophyll-a values at ebb and flood tide.
- (3) Colour-coded maps of morning and afternoon surface chlorophyll-a concentrations of the entire study area created by applying the statistical models developed from 30 point samples.

Multispectral data from the Daedalus 1260 scanner (or TM) can be used to map horizontal distributions of phytoplankton biomass (chlorophyll-a) in shallow and turbid waters such as northern San Francisco Bay. A simple regression model that uses count values from four wavebands can predict chlorophyll-a distribution almost as accurately as field techniques based upon measurement of *in vivo* fluorescence. During this study, for example, we measured *in vivo* fluorescence (Turner Designs Model 10 fluorometer) from surface samples collected at sites 4, 7, 8, 9, 10, 11, 12 and 13 during five stages of the tide on 28 August. Linear regression of chlorophyll-a against *in vivo* fluorescence is a common method for predicting chlorophyll-a, and in this instance the fit of chlorophyll-a to *in vivo* fluorescence (see figure 9) showed only 8 per cent improvement which was not much better than that of fits to Daedalus MSS data.



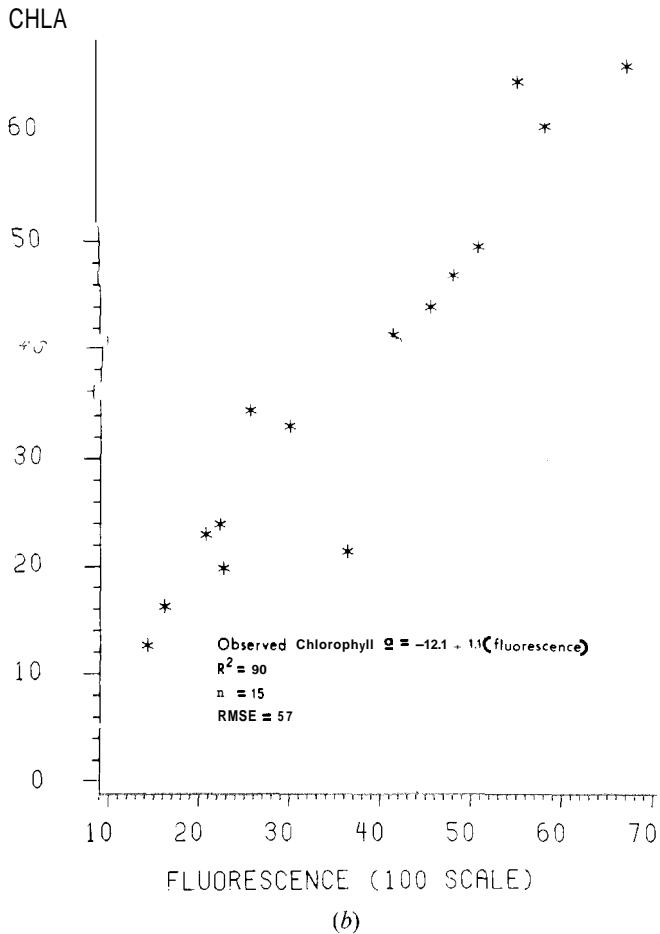


Figure 9. (a) Plot of observed chlorophyll-a concentrations ($\mu\text{g/l}$) versus model predictions for sites 4, 7, 8, 9, 10, 11, 12 and 13 using both morning and afternoon data. (b) Plot of observed chlorophyll-a concentrations ($\mu\text{g/l}$) versus fluorescence for sites 4, 7, 8, 9, 10, 11, 12 and 13 as recorded by a continuous shipboard fluorometer for both ebb and flood tide.

Predicted horizontal distributions of chlorophyll-a (figure 8) are consistent with gross horizontal distributions inferred from boat sampling. For example, field sampling has consistently shown that chlorophyll concentration is highest in discrete samples collected over the northern shallows of Suisun Bay than in the deeper channels (Cloern et al. 1983) and that chlorophyll concentration is usually higher in that reach of the channel adjacent to the northern shoals. Both of these features are apparent from Daedalus imagery, but the spatial resolution available from the application of remote sensing is much greater than has been possible from field surveys. Thus, results of this study offer the first accurate views of the two-dimensional structure of phytoplankton distribution in this estuary. Moreover, sequential flyovers provide a tool for examining the dynamic nature of the phytoplankton maximum. For example, the tidal advection of high-chlorophyll water from the northern shoals into the main body of Suisun Bay on low (flood) tide is apparent (figure 8) and this spatial pattern is consistent with the hypothesis that shallow waters are the source of new phytoplankton biomass (Cloern et al. 1983).

7. Conclusions

The results of this investigation indicate:

(1) The TM on board LANDSAT may provide repetitive coverage of this estuary in the wavelength regions applicable to predicting chlorophyll-a concentrations. Band transformations of TM data that correspond to Daedalus 1260 channels 3 minus 10 and ratio of 7 to 8 are TM channel 1 minus 5 (0.45–0.52 to 1.55–1.65 μm) and ratio of channels 3 (0.63–0.69 μm) to 4 (0.76–0.90 μm), respectively.

(2) Surface concentrations of chlorophyll-a can be predicted utilizing information in the visible and near-infrared wavelength regions of a Daedalus 1260 MSS regardless of tidal state. The spectral resolution of this scanner was extremely useful in recording wavelength regions influenced primarily by chlorophyll-a. At the same time, the spatial resolution of this scanner increases the capability of detecting more detailed local variations in surface chlorophyll-a concentrations compared with the LANDSAT MSS system.

(3) Results of this study show the potential for TM multispectral data as a tool for monitoring water quality (including chlorophyll-a) and for studying hydrodynamic/biological features of estuaries. However, routine application of the method is not realistic until the significance of potential problems has been resolved. For example, problems with bottom reflectance or reflectance from exposed mudflats, particularly where chlorophyll concentrations are high in sediments, cannot be ignored. This is true for northern San Francisco Bay (Thompson *et al.* 1981), and the predicted high chlorophyll values around the perimeter of Suisun Bay (figure 7) may be invalid because of this source of error. Also, problems arise with tidal currents—the tidal excursion along northern San Francisco Bay is about 10 km, and water parcels are advected rapidly during the course of sampling from boats. Therefore, care must be taken to ensure simultaneous collection of surface truth and remotely sensed data, particularly in waters with strong tidal currents.

(4) In this investigation, model coefficients were similar but not conservative from the morning to the afternoon. Atmospheric correction of data based on surface measured upwelling and downwelling irradiance at various sites during data collection would allow calibration of solar input from morning to afternoon and could possibly contribute to coefficient standardization.

(5) All regression models explained a significant portion of the variability of the measured surface concentration of chlorophyll-a. Standard errors of the regression of continuous fluorometric surface traces versus acetone-extracted laboratory measures of chlorophyll-a are similar to standard errors predicted using remote-sensing techniques. Larger sample sizes will be necessary to verify functional models.

(6) Further investigation is necessary to confirm the applicability of the model for different times of year and in different regions of San Francisco Bay. The success of using Daedalus MSS data for defining chlorophyll-a distributions in this study may, in part, result from the relatively homogeneous phytoplankton community composition in the study area. Different models may be needed to predict surface chlorophyll-a concentrations at different times of year or for a much different part of the bay (*i.e.* south San Francisco Bay) where phytoplankton species and dynamics differ considerably from the study area. Present knowledge of the actual temporal and spatial variations in phytoplankton dynamics is an essential input in developing a tailored remote-sensing system capable of monitoring conditions for a local geographic region.

Acknowledgments

The research leading to this manuscript was sponsored in part by NOAA, National Sea Grant College Program, Department of Commerce, under grant number NA80AA-D-00120, project number R/CZ 68, through the California Sea Grant College Program, in part by the California State Resources Agency, and in part by the Water Resources Division of the U.S. Geological Survey. The U.S. Government is authorized to produce and distribute for governmental purposes.

We thank J. Arthur of the U.S. Bureau of Reclamation, H. Proctor of the California Department of Water Resources, M. Eldridge of the Tiburon Marine Laboratory and M. Kjelson and P. Herrgasell of the California Department of Fish and Game for making the surface measurements available to us for this project.

The authors would like to thank R. N. Colwell of the University of California, Berkeley, for his overall advice on this research, R. Wrigley of the NASA Ames Research Center for arranging the acquisition of Daedalus multispectral data and A. Kaugars and P. Ritter of the Remote Sensing Research Program of the University of California, Berkeley, for their assistance in data processing. We also thank Kimberley Moss of the Computer Graphics Center of North Carolina State University for her assistance in preparation of this manuscript.

References

- ANDERSON, H. M., and HORNE, A. J. 1975, Remote sensing of water quality in reservoirs and lakes in semi arid climates. SERL Report No. 75-1, University of California, Berkeley, NASA Grant No. NSG-2003, p. 132.
- BOWKEK, D. E., HARDESTY, C. A., and JOBSON, D. J., 1983, Remote sensing of sediment and chlorophyll with the test-bed aircraft multispectral scanner. NASA Technical Memorandum TM:85490, Washington, D.C., pp. 1-23.
- CLOERN, J. E., ALPINE, A. E., COLE, B. E., WONG, R. L. J., ARTHUR, J. F., and BALL, M. D., 1983, River discharge controls phytoplankton dynamics in the northern San Francisco Bay estuary. *Estuar. Coastal shelf Sci.*, 16, 415.
- CLOERN, J. E., and CHENG, R. T., 1981. Simulation model of *Skeletonema costatum* population dynamics in northern San Francisco Bay, California. *Estuar. Coastal shelf Sci.*, 12, 83.
- CONOMOS, T. J., 1979, Properties and circulation of San Francisco Bay waters. In *San Francisco Bay: The Urbanized Estuary*. edited by T. J. Conomos (American Association for the Advancement of Science), pp. 47-84.
- CONOMOS, T. J., and PETERSON, D. H., 1977, Suspended-particle transport and circulation in San Francisco Bay: an overview. In *Estuarine Processes*, Vol. 2, edited by M. Wiley (New York: Academic Press), pp. 82-97.
- FARMER, F. H., Jarrett, O., Jr., and BROWN, C. A., JR., 1983, Visible absorbance spectra: a basis for *in situ* and passive remote sensing of phytoplankton concentration and community concentration. NASA Technical Paper TP-2094, Washington; D.C., pp. 1-32.
- GORDON, H. R., and CLARK, D. K., 1980, Atmospheric effects in remote sensing of phytoplankton pigments. *Boundary-Layer Met.*, 18, 299.
- GREW, G. W., 1981, Real-time test of MOCS algorithm during Superflux 1980. In *Chesapeake Bay Plume Study: Superflux 1980*, edited by J. W. Cambell and J. P. Thomas, Proc. NASA Conf. 2188, pp. 301-322.
- JOHNSON, R. W., 1978, Mapping of chlorophyll-a distribution in coastal zones. *Photogramm. Engng remote Sensing*, 44, 617.
- JOHNSON, R. W., BAHN, G. S., and THOMAS, J. P., 1981, Synoptic thermal and oceanographic parameter distributions in the New York Bight Apex. *Photogramm. Engng remote Sensing*, 38, 1593.
- KHORRAM, S., 1981 a, Use of Ocean Color Scanner data in water quality mapping. *Photogramm. Engng remote Sensing*, 47, 667.
- KHORRAM, S., 1981 b, Water quality mapping from Landsat digital data. *Int. J. remote Sensing*, 2, 145.

- KIM, H. H., McCLAIN, C. R., and BLAINE, L. R., 1980, Ocean chlorophyll studies from a U-2 aircraft platform. *J. geophy. Res.*, 85, 3892.
- MEADE, R. H., 1972, Transport and deposition of sediments in estuaries. *Mem. geol. Soc. Am.*, 133, 91.
- MOREL, A., and PRIEUR, L., 1977, Analysis of variations in ocean color. *Limnol. Oceanogr.*, 22, 709.
- MUNDAY, J. C., and ZUBKOFF, P. L., 1981, Remote sensing of dinoflagellate blooms in a turbid estuary. *Photogramm. Engng remote Sensing*, 47, 523.
- PETERSON, D. H., CONOMOS, T. J., BROENKOW, W. W., and SCRIVANI, E. P., 1975, Processes controlling the dissolved silica distribution in San Francisco Bay. In *Estuarine Research*, Vol. 1, edited by L. E. Cronin (New York: Academic Press), pp. 153–187.
- POSTMA, H., 1967, Sediment transport and sedimentation in the estuarine environments. In *Estuaries*, Vol. 83, edited by G. H. Lauff (American Association for the Advancement of Science), pp. 158–179.
- STRICKLAND, J. D. H., and PARSONS, T. R., 1972, *A Practical Handbook of Seawater Analysis*. Fisheries Research Board of Canada Bulletin, 167, 310 pp.
- THOMPSON, J. K., NICHOLS, F. H., and WIENKE, S. M., 1981, Distribution of benthic chlorophyll in San Francisco Bay, California, February 1980–February 1981. U.S. Geological Survey Open-File Report 81–1134, Menlo Park, CA, U.S.A.
- UNO, S., SUGAHARA, U., and HAYAKAWA, S., 1980, Remote sensing of chlorophyll found in bodies of water. *Proceedings of the 14th International Symposium on Remote Sensing of the Environment*, Ann Arbor, Michigan, pp. 1147–1157.
- WILSON, W. H., and KIEFER, D. A., 1979, Reflectance spectroscopy of marine phytoplankton. Part 2. A simple model of ocean color. *Limnol. Oceanogr.*, 24, 673.
- YENTSCH, C. S., 1960, The influence of phytoplankton pigments on the colour of sea water. *Deep-Sea Res.*, 7, 1.